Cryo-TEMPO

Algorithm Theoretical Basis Document

Land Ice

Prepared by	:	Alan Muir	29/09/2022
Checked by	:	Stefan Hendricks	21/11/2022
Approved by	:		

Change Log

Issue	Author	Affected Section	Change	Status
0	A. Muir	All	Document Creation	Complete
1.1	A. Muir	All	Version 1 Content	Complete
2.1	Land Ice Team	All	Version 1 Revisions	In Review

Acronyms and Abbreviations

AD	Applicable Document
ADF	Auxiliary Data File
AO	Announcement of Opportunity
ATBD	Algorithm Theoretical Basis Document
COG	Centre of Gravity
CS2	CryoSat-2
DEM	Digital Elevation Model
EPSG	European Petroleum Survey Group
ESA	European Space Agency
GSFC	Goddard Space Flight Centre
IMBIE	Ice Sheet Mass Balance Intercomparison Exercise
L1	Level-1
L2	Level-2
LRM	Low Resolution Mode
MSSL	Mullard Space Science Laboratory (part of UCL)
OCOG	Offset Centre Of Gravity retracker
PEG	Polar Expert Group
POCA	Point of Closest Approach
RA	Radar Altimetry
RD	Reference Document
REMA	Reference Elevation Model of Antarctica
SAR	Synthetic Aperture Radar
SIN	Synthetic Aperture Radar Interferometric
SIRAL	SAR Interferometric Radar Altimeter
SoW	Statement of Work
TCOG	Threshold Centre of Gravity
TDP	Thematic Data Product
TDS	Test Data Set
TFMRA	Threshold First Maximum Retracker Algorithm
TN	Technical Note
UCL	University College London
WGS	World Geodetic System

Table of Contents

1 INTRODUCTION

1.1 Purpose and Scope

This document comprises the Algorithm Theoretical Basis Document (ATBD) for the Baseline-B Land Ice products of the *CryoSat-2 ThEMatic PrOducts* (*Cryo-TEMPO*) study (phase 2.1), Ref: ESA AO/1-10244/2-/I-NS. The ATBD has been written by MSSL (UCL), with contributions from all members of the Cryo-TEMPO consortium. Lancaster University as the prime contractor is the contact point for all communications regarding this document.

The Algorithm Theoretical Basis Document (ATBD) provides a high-level description of the algorithms and processing used to produce each Cryo-TEMPO Baseline-B land ice product parameter.

1.2 Document Structure

The document is structured as follows:

- Section 1 – Introduction
- Section 2 – Baseline Change Log
- Section 3 – Land Ice Parameters
- Section 4 – Overall Land Ice Processing Flow
- Section 5 – Algorithm Descriptions
- Section 6 – Uncertainty Estimate Table Creation
- Section 7 – Examples
- Section 8 – Known Issues

1.3 Applicable and Reference Documents

Applicable documents

Reference	Title
AD1	Statement of Work ESA Express Procurement Plus - EXPRO+ CryoSat-2 ThEMatic PrOducts | Cryo-TEMPO, Issue 1, Revision 0, Date of Issue 01/04/2020 [Ref. ESA-EOPG-EOPGMQ-SOW-10].
AD2	Invitation to Tender for CryoSat-2 ThEMatic PrOducts | Cryo-TEMPO REF.: ESA AO/1-10244/2-/I-NS [Ref. SA-IPL-POE-NS-sp-LE-2020-313].

Reference documents

Reference	Title
RD1	Copernicus Polar and Snow Cover Applications User Requirements Workshop, http://www.copernicus.eu/polar-snow-workshop
RD2	PEG-1 Report, User Requirements for a Copernicus Polar Mission, Step 1 Report, Polar Expert Group, Issue: 12th June 2017
RD3	PEG-2 Report, Polar Expert Group, Phase 2 Report on Users Requirements, Issue: 31st July 2017
RD4	CryoSat2 : L2 Design Summary Document. CS-DD-MSL-GS-2002
RD5	Guidelines for reverting Waveform Power to Sigma Nought for CryoSat-2 in SAR mode. XCRY-GSEG-EOPS-TN-14-0012

2 BASELINE CHANGE LOG

This section details the main changes between each Cryo-TEMPO Land Ice processing baseline. A processing baseline is the fixed state of the algorithms, auxiliary data, configuration files and processing software used to process the full mission from ESA L1b files through to Cryo-TEMPO land ice products.

2.1 Baseline-A

Baseline-A was the first Cryo-TEMPO land ice product, released in January 2022.

2.2 Baseline-B

Scheduled for release in January 2023.

Algorithm	Description of change
SARin Retracking	A new Maximum Coherence Retracker replaces TCOG retracker for SARin waveforms only.
LRM Retracker (TCOG)	Smoothing of waveforms changed from sliding average (width=3) to Savitsky-Golay (width 9)
Backscatter (SARin)	No algorithm changes, but a change in the SARin retracker causes an ~2dB mean change in the backscatter calculated for SARin measurements as compared to Baseline-A. This is expected as the returned power relates to a new retracking point which will be on average higher up the waveform leading edge (than chosen by the Baseline-A TCOG retracker with a 50% threshold).
SARin Across-track Angle Calculation	The phase difference waveform is now sampled at the location of maximum coherence chosen by the retracker (instead of using a model fit in Baseline-A). No smoothing or interpolation is performed. The phase difference value is then converted into an angle from the boresight vector (given in the L1 data).
SARin Phase Unwrapping and Ambiguity Detection	In Baseline-A an ambiguity check was performed to detect potential phase wrapping by comparing the measured SARin height with an external DEM. Differences greater than 100m were flagged as ambiguous but no attempt was made to correct the measurements location and elevation. In Baseline-B to determine if the original phase measurement was wrapped, the phase difference is then unwrapped and a second elevation and location is calculated. The location with the smallest difference from

	the DEM is taken as the POCA and the height measurement is given at that location. This results in the retrieval of a higher number of SARin measurements over the ice sheet margins in Baseline-B.
Glaciological Drainage Basins	An additional glaciological drainage basin parameter has been added to the product (netcdf 'basin2' parameter). This provides the basin number according to Rignot (2016). Previously only the basins defined by Zwally (2012) were provided in the 'basin' parameter. Both these drainage basin definitions are widely used and are specified by the IMBIE project for ice sheet mass balance calculations.
Uncertainty	The uncertainty parameter is now calculated from the statistics of differencing closely located elevation measurements from Cryo-TEMPO and IceSAT-2 ATL-06 v005 per band of surface slope. In Baseline-A the uncertainty was calculated from the statistics of Cryo-TEMPO crossover differences per band of surface slope. In both cases the statistics are generated from combining differences less than 1 month over a single reference year (2020).

3 LAND ICE PARAMETERS

3.1 Parameter Definition

This section describes the main land ice parameters contained in the Cryo-TEMPO Land Ice Thematic Data Product (TDP). Cryo-TEMPO land ice products contain measurements along the CryoSat-2 orbit track (at a rate of 20 measurements per second) and are not gridded.

Parameter	Description	Units
Latitude (POCA)	Latitude of estimated echo location (Point Of Closest Approach) [-90,+90]. Positive latitude is North latitude, negative latitude is South latitude. In LRM/SARIn modes, it may deviate from nadir due to slope correction or interferometry.	degs (N)
Longitude (POCA)	Longitude of estimated echo location (Point Of Closest Approach) [-180,+180]. East longitude relative to Greenwich meridian. In LRM/SARIn modes, it may deviate from nadir due to slope correction or interferometry.	degs (E)
Elevation (of land ice surface (grounded and floating ice)	Measured height of the surface above the reference ellipsoid (WGS84) at the coordinate location [longitude] [latitude], computed using the TCOG retracker for LRM mode measurements or the Maximum Coherence Retracker for SARin mode. All instrumental and appropriate geophysical corrections included. Corrected for surface slope via a slope model in LRM mode. Corrected for surface slope via phase information in SARIn mode.	m
Backscatter (also known as sigma0)	The measured backscatter from the surface, corrected for instrument effects, and including a system bias that calibrates the results against previous missions. The backscatter is computed from the amplitude of the waveform in Watts, as measured by the retracker. The measured power is used to solve the radar equation to recover the value for backscatter.	dB
Uncertainty of Elevation	Contains an estimate of the uncertainty of each Elevation measurement.	m

Measurement Mode	The mode that the CryoSat-2 SIRAL instrument was in when each measurement was taken (LRM, SARin, or SAR)	flag
Surface Type	For each location a flag indicates the type of surface over which the measurement of elevation was taken. Surface types are: ocean, ice free land, grounded ice, or floating ice. The surface type is derived from an external ice sheet specific dataset from BedMachine Antarctica (v2) and BedMachine Greenland (v3).	flag
DEM Elevation	Reference elevation at each measurement location interpolated from an external high resolution Digital Elevation Model (ArcticDEM v3 for Greenland, REMA v1.1 for Antarctica).	m
Glaciological Catchment Identifier Number (Zwally 2012)	Each Cryo-TEMPO elevation measurement has associated with it a glaciological catchment identifier, the purpose of which is to allow the user to easily filter by – and extract data from – a specific basin or catchment of interest. Catchments are the same as used in http://imbie.org as originally defined by Zwally (2012).	integer
Glaciological Catchment Identifier Number (Rignot 2016) : new parameter in baseline-B	Each Cryo-TEMPO elevation measurement has associated with it a glaciological catchment identifier, the purpose of which is to allow the user to easily filter by – and extract data from – a specific basin or catchment of interest. Catchments are the same as used in http://imbie.org as originally defined by Rignot (2016).	integer

3.2 Geographical Coverage

The Cryo-TEMPO thematic land ice product covers both the Greenland and Antarctic Ice Sheets, incorporating both their grounded and floating (ice shelf) sectors. Measurements are processed if they are within 10km of the grounded or floating ice mask as defined by the following Bedmachine surface type masks:

- BedMachine v2 Antarctica (https://nsidc.org/data/nsidc-0756/versions/2).
- BedMachine v3 Greenland (https://nsidc.org/data/idbmg4).

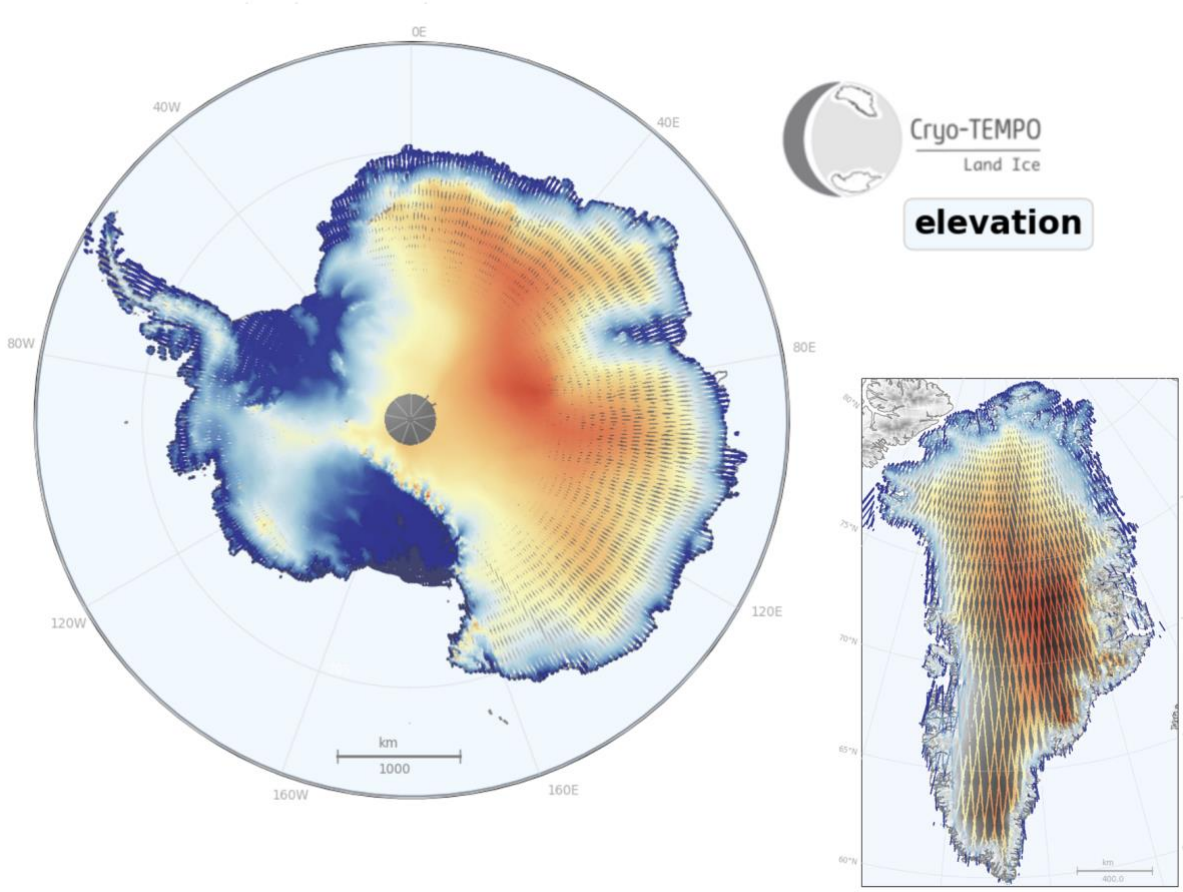

Figure 1. Geographical coverage of the Cryo-TEMPO thematic land ice product (elevation parameter shown).

4 OVERALL LAND ICE PROCESSING FLOW

The land ice processing chain is formed from 3 separate sub-processors. The primary inputs to stage 1 are available ESA CryoSat L1b Baseline-D/E files from the full mission archive. For each L1b file that contains measurements inside a grounded or floating ice mask surrounding Antarctica or Greenland a CryoTEMPO product file is finally output in stage 3.

In the first stage the products are masked for land ice areas and the main geophysical parameters (elevation and backscatter), the surface type, and the measurement geolocation are calculated for each record of each L1b file.
The second stage is performed only once on a year of intermediate elevation data and coincident ICESat-2 ALT-06 elevation measurements. The second stage calculates an uncertainty table per band of slope.
In the final stage, the uncertainty, glaciological basins, and DEM values are interpolated for each record and the Cryo-TEMPO land ice product files are created.

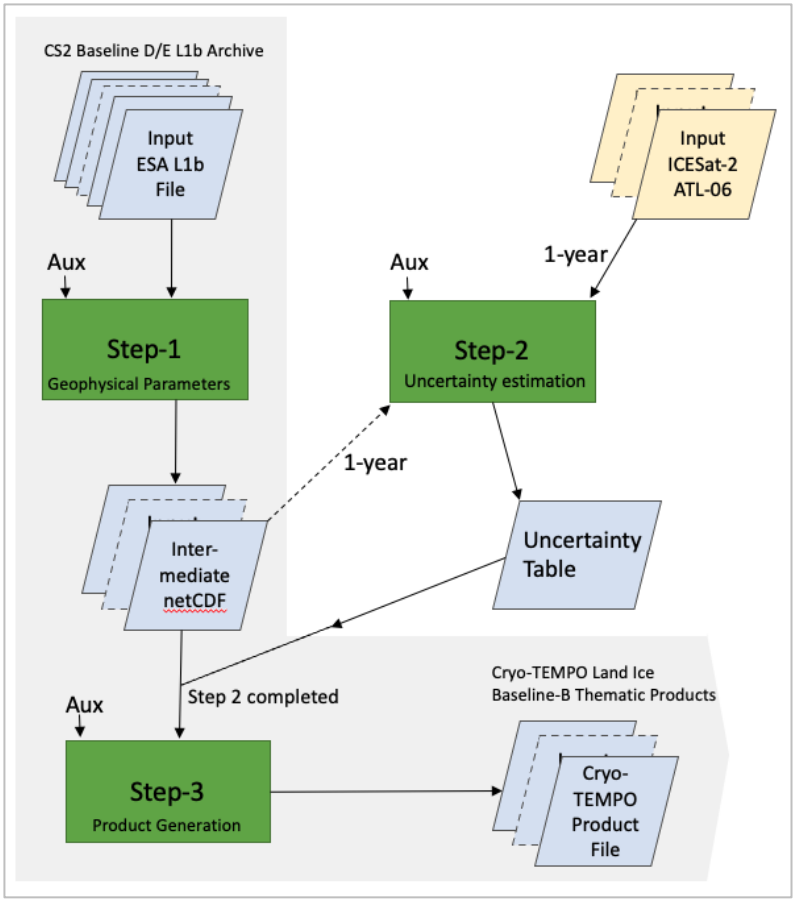

Figure 2. Overall Land Ice Processing Flow Diagram.

Each stage can be further decomposed into individual algorithms as shown in Figure 3.

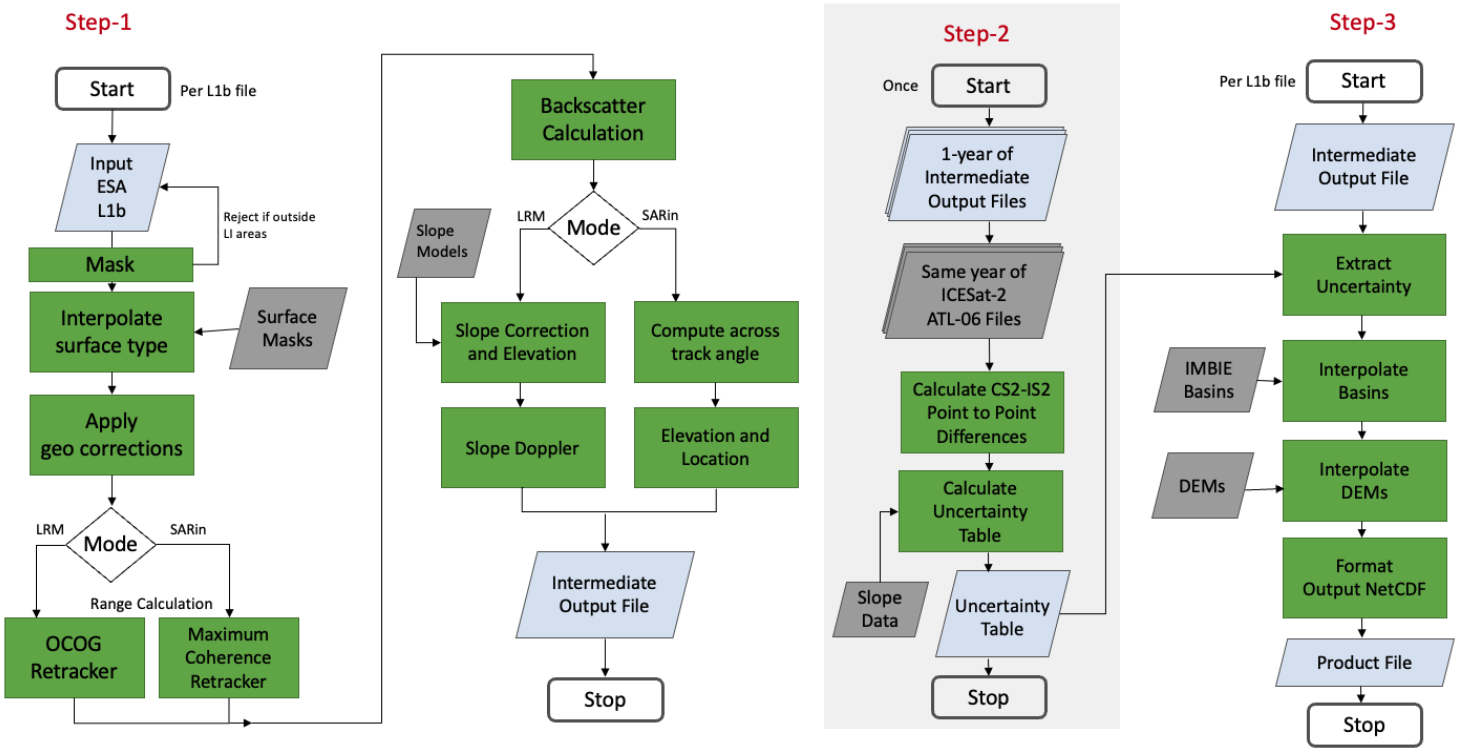

Figure 3. Detailed Land Ice Processing Flow Diagram.

4.1 Stage-1 Processing

The first stage of the Cryo-TEMPO Land Ice processing reads in a L1b file and performs the following processing steps:

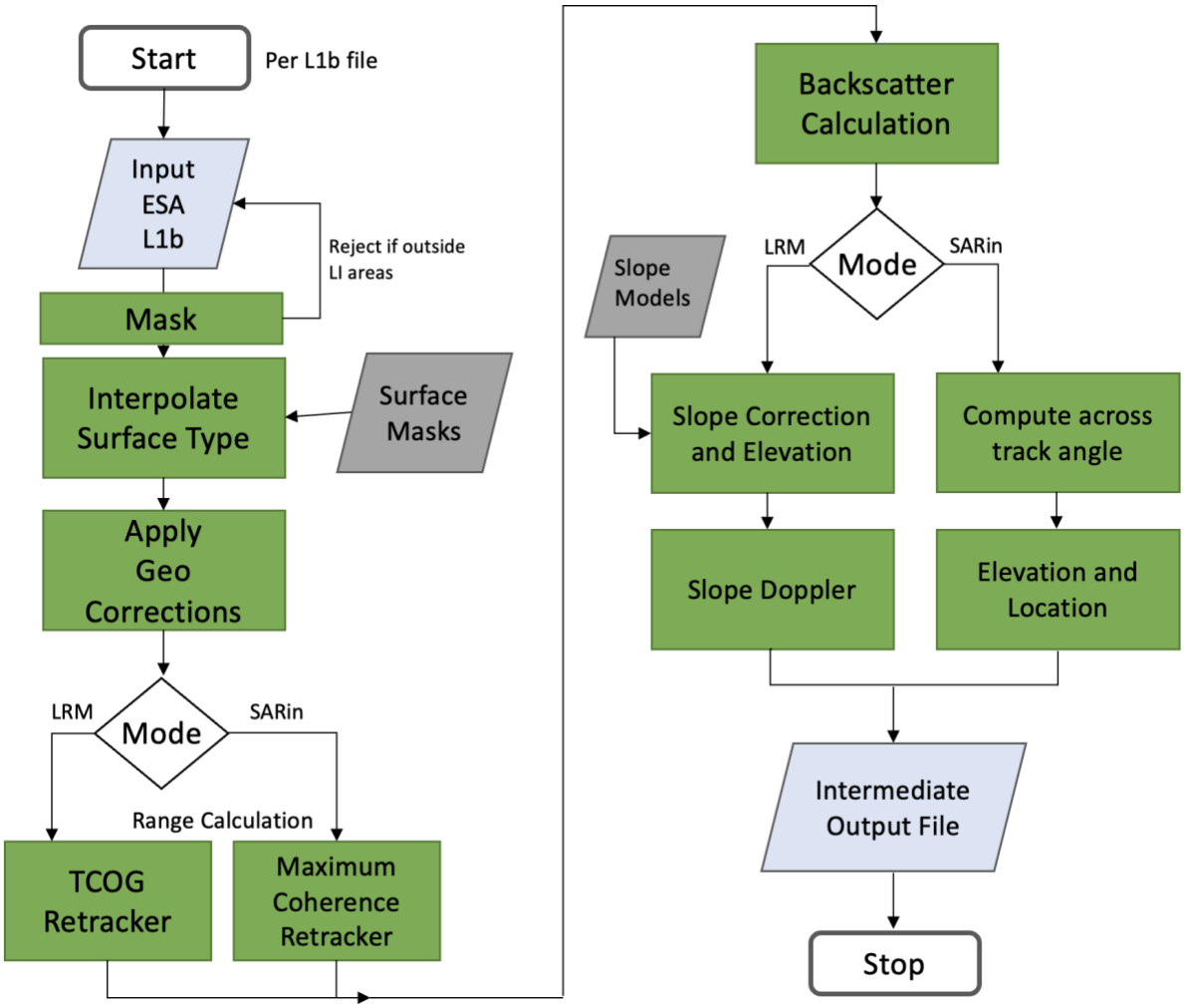

Figure 4: Stage 1 Processing Overview

- Test files for measurement locations inside an Antarctic and Greenland mask (10km from the coastline or floating ice shelves). If there are no suitable measurements, file is rejected.
- For each location surface type is extracted from an auxiliary data source.
- Geophysical corrections are summed based on surface type.
- Retracking corrections
    - TCOG Retracker for LRM mode measurements.

    - Maximum Coherence Retracker for SARin mode measurements. The Maximum Coherence Retracker is new in Baseline-B.
- Backscatter calculation.
- Fully corrected range calculation.
- Geolocation: Computation of POCA (point of closest approach) location is a different process for LRM and SARin modes.
    - LRM – Low Resolution Mode
        - Slope model correction.
        - Computation of offset location, and height at that location.
        - Correction of height by a slope doppler corrections.

    - SARIn – SAR Interferometric mode (also known as SIN mode)
        - Computation of the across track angle from the phase waveform.
        - Computation of the offset location, and height at that location.
        - Phase unwrapping.
- Computation of elevation.

The stage-1 processor then generates a partially filled Cryo-TEMPO netCDF format output product file which is used as input to both stages 2 and 3.

4.2 Stage-2 Processing

The second stage of the Cryo-TEMPO Land Ice processor generates the uncertainty tables.

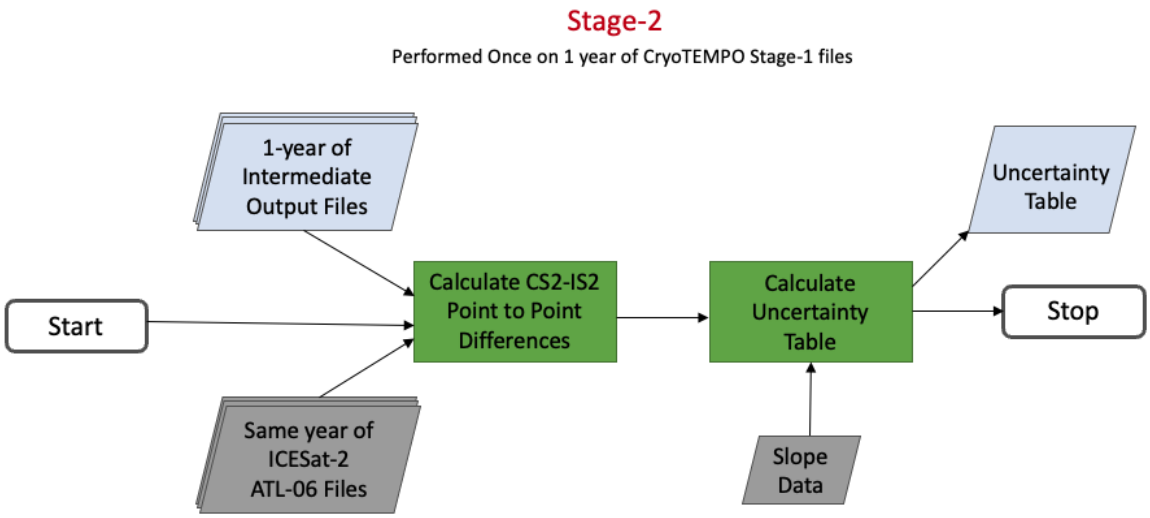

Figure 5: Stage-2 Processing Overview

- This processor is run on a 1-year period (2020) of Cryo-TEMPO stage-1 data.
- Calculating the point to point elevation differences between closely located Cryo-TEMPO measurements and ICESat-2 ATL-06 measurements.
- Finds the surface slope at each Cryo-TEMPO location from an external ADF.
- Calculates the uncertainty table from the median of absolute differences in each 0.1 degree slope band between 0 and 2 degrees of slope.
- The processor outputs a table of expected uncertainty as a function of surface slope.

4.3 Stage-3 Processing

The final stage of the Cryo-TEMPO Land Ice processor adds the required parameters to the Cryo-TEMPO output files.

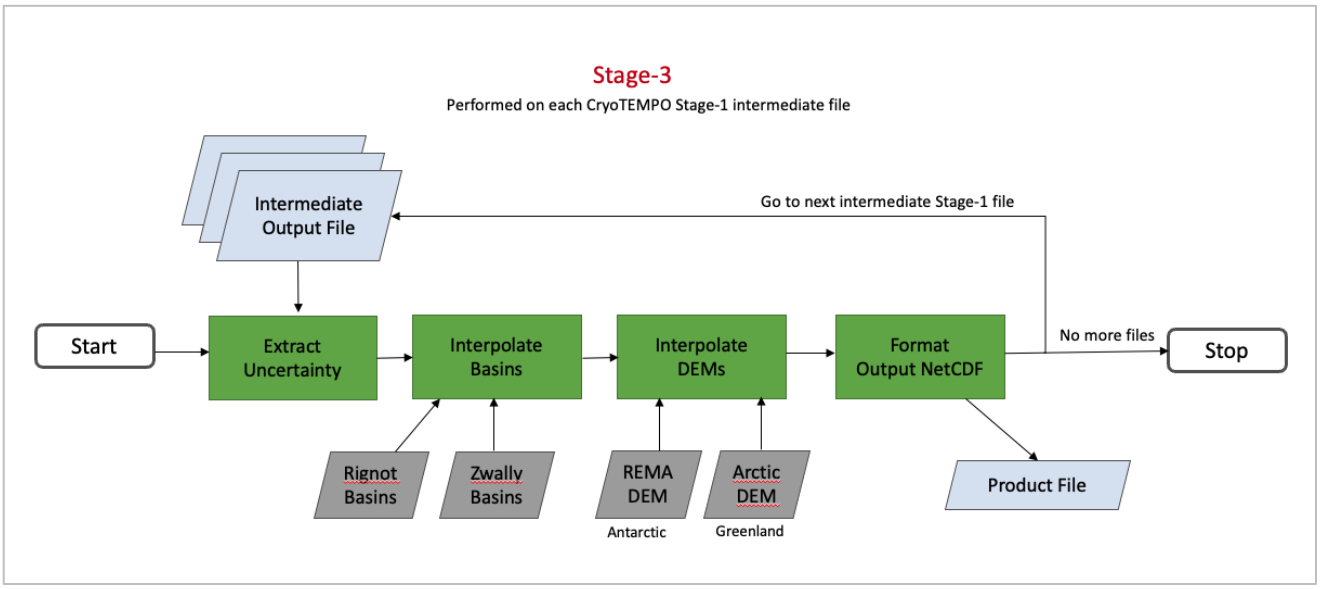

Figure 6: Stage 3 Processing Overview

- Extraction of the Zwally and Rignot basin IDs at each POCA location from external Auxiliary Data File (ADF).
- Extraction of the Digital Elevation Model (DEM) height value at each POCA location, interpolated from external ADF (REMA for Antarctica or ArcticDEM for Greenland).
- Extraction of uncertainty based on surface slope at each POCA location from the uncertainty tables generated in Stage-2.
- New netCDF variables are created in the product for each of the new Stage-3 parameters.

5 ALGORITHM DESCRIPTIONS

This section provides details of the main processing steps and algorithms used in the Cryo-TEMPO Land Ice processor. For efficiency we focus on providing full details for the new algorithms that are implemented within the frame of Cryo-TEMPO, whereas for existing algorithms (used in ESA Baseline D/E L2 processing) we provide a summary and refer the reader to the relevant documentation where the full details are given.

5.1 Surface Type Masks

The source of the surface type mask data are external netCDF mask files from:

- BedMachine v2 Antarctica (https://nsidc.org/data/nsidc-0756/versions/2).
- BedMachine v3 Greenland (https://nsidc.org/data/idbmg4).

The surface type masks are netCDF format grids of surface type in stereographic projection (EPSG:3031 for Antarctic masks, EPSG:3413 for Greenland).

To identify the surface type value for each 20 Hz nadir location, the value of the mask corresponding to the grid cell (indexed by nearest neighbour) in which the 20 Hz record falls is found.

(X_0, Y_0) = grid corner from netCDF file
Step = grid spacing from netCDF file

20 Hz nadir Latitude (lat_20_ku) and Longitude (lon_20_ku) are reprojected to (X,Y) coordinates in the polar stereographic projection of the surface type masks.

The surface type of the input masks for each nadir location is found from:

$$surface\_type\_20\_ku = grid\left[\frac{round(X - X_0)}{step}, \frac{round(Y - Y_0)}{step}\right]$$

Input surface type mask values are:

0 = ocean
1 = ice-free land
2 = grounded ice
3 = floating ice
4 = Lake Vostok (Antarctic mask), non-Greenland land (Greenland mask)

The surface type mask value is then mapped to the Cryo-TEMPO surface type specification (dependant on hemisphere) of:

Antarctica:

- 0 -- ocean (source value 0)
- 1 -- grounded ice (source values 2 (grounded Ice) and 4 (Lake Vostok))
- 2 -- floating ice (source value 3)
- 3 -- ice free land (source value 1)

Greenland:

- 0 -- ocean (source value 0)
- 1 -- grounded ice (source value 2)
- 2 -- floating ice (source value 3)
- 3 -- ice free land (source value 1)
- 4 -- non-Greenland land (source value 4)

5.2 Retracking

Waveform retracking is the process of correcting (fine tuning) the satellite range measurement to the point of closest approach on the ice surface by finding the departure of the waveform leading edge from the altimeter tracking range gate.

Waveform returned by each CryoSat instrument modes (LRM or SARin) over land ice have quite different typical characteristics and operate over different topographical surface types: LRM over the smoother and flatter interior ice sheets, and SARin over rougher and more topographically variable terrain with a higher slope. Due to these significant differences, it is beneficial to use different retracking techniques for each mode. To choose the best retracker and retracking parameters for each instrument mode the Cryo-TEMPO project selects the latest retracking algorithms recommended by the very latest published and peer reviewed studies and performs a round robin comparison of the resulting elevation measurements in comparison to available validation data (from ICESat-2 and Operation ICEBridge). The retracking algorithms and settings that provide the closest match in accuracy and precision to the validation data are selected.

For LRM waveforms, the TCOG retracker (McMillan et al, 2019) was selected, and for SARin waveforms a Maximum Coherence retracker (derived from Aublanc et al, 2021).

5.2.1 TCOG Retracker

The TCOG retracker is a threshold retracker (McMillan et al., 2019) adapted from the Offset Centre of Gravity (OCOG) method proposed by Wingham et al., 1986, and the TFMRA retracker (Helm et al., 2014). Instead of using the OCOG centre of gravity (COG) and OCOG width to find the leading edge position, the TCOG method identifies the leading edge (LE) from the first maxima (above a normalised threshold), and then finds the first index on the LE above a tuneable percentage of the OCOG amplitude (Figure 7).

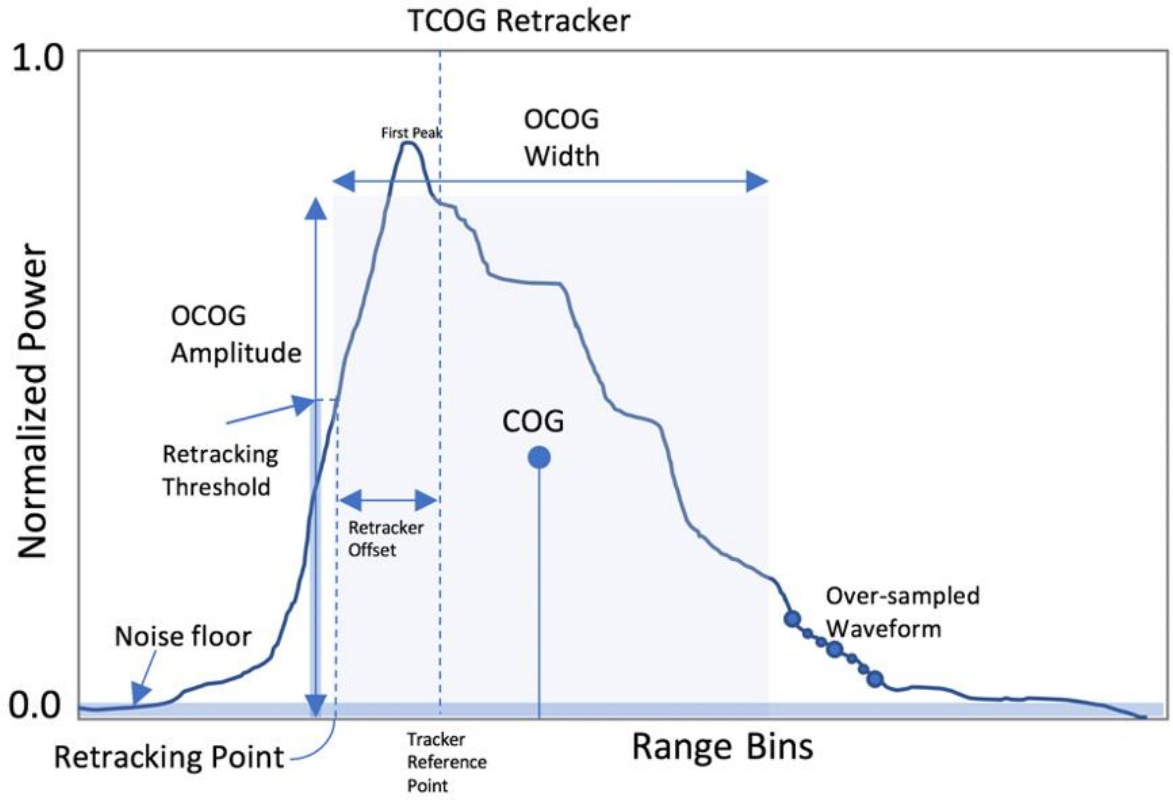

Figure 7: Schematic description of the TCOG retracker.

The specific implementation of the TCOG retracker for the Cryo-TEMPO Land Ice processor uses the following tuneable parameters and processing steps.

5.2.1.1 Tuneable Constants

Tuneable Parameter	Symbol	Value
Speed of Light	C	299792458 m/s
Chirp bandwidth	B	320000000 Hz
Waveform Oversampling Factor	W_s	100
Noise Sampling Limit	N_s	6
Noise threshold	P_{noise_max}	0.3
Leading Edge Threshold	L_t	0.05
Leading Edge Normalised Amplitude Threshold	A_s	0.2
Savitsky-Golay Smoothing width	S_w	9
Savitsky-Golay Polynomial Order	S_p	3

Retracking Threshold	R_t	0.2 (LRM)
Reference bin number	I_{ref}	64 (LRM), 512 (SIN)
Range bin size	R_b	C/(2B) for LRM C/(4B) for SIN

5.2.1.2 Retracking Method

The following retracking steps are applied to each waveform:

1. Compute maximum amplitude of waveform power, *P*.

2. Compute Normalised waveform, P_n, so that maximum amplitude is 1.

3. Apply a 1-d Savitsky-Golay smooth to the waveform, forming P_{n_smooth}.

4. Compute thermal noise, P_{Noise}, from first N_s samples of the normalised waveform:

$$mean(\, P_n[0{:}\, N_s] \,)$$

5. Reject the waveform if thermal noise is greater than threshold P_{noise_max}.

6. Over-sample the normalised waveform P_n and normalised smoothed waveforms P_{n_smooth} by the over-sampling factor W_s using 1-d linear interpolation, forming P_{n_i} and $P_{n\_smoothed\_i}$.

7. Compute the first derivative, *D*, of the smoothed waveform $P_{n\_smooth\_i}$ using a central difference which is calculated between *i-1:i+1*. The gradient is computed using second order accurate central differences in the interior points and first order accurate one-sides (forward or backwards) differences at the boundaries.

8. Find a suitable leading edge, by performing an iterative search:
   a. Find $i_{leading\_edge\_start}$, the first waveform index where:

$$P_{n\_smooth\_i} > (P_{noise\_max} + L_t)$$

   and

$$D_i > 0$$

   b. Find the peak of the leading edge, i_{peak}, defined as where the gradient D_i first becomes negative after the power threshold is exceeded.

c. Calculate the amplitude of the peak:

$$A_{peak} = i_{peak} - i_{leading\_edge\_start}$$

d. If $A_{peak} > A_s$ then go to next step (leading edge is found), else continue search for leading edge.

9. Compute the OCOG amplitude, *A*:

$$A = \left(\sum_{i=1+n}^{N-n} P_i^4(t) \Big/ \sum_{i=1+n}^{N-n} P_i^2(t) \right)^{1/2}$$

10. Compute a proportion of the Amplitude A, using the retracker threshold R_t (R_t is a mode (LRM, SIN) dependent threshold):

$$R_{tcog} = R_t A$$

11. Find the first leading edge value i_{tcog} above the retracking threshold for the unsmoothed waveform.

12. Compute range offsets from reference to retracked bins:

$$i_{offset} = i_{tcog} - i_{ref}$$

13. Convert range offset to m:

$$R_{offset} = i_{offset} R_b$$

14. Store power in counts at the retracking point (used for the backscatter calculation):

$$P_{rtr} = P\left[i_{tfmra}\right]$$

5.2.2 Maximum Coherence SARin Retracker

The Maximum Coherence SARin Retracker is based on a method of leading-edge detection (McMillan 2019), waveform smoothing, and retracking point selection by maximum coherence (Aublanc et al., 2021).

5.2.2.1 Leading Edge Selection

The waveform leading edge is first selected using an identical method to that used in the TCOG retracker.

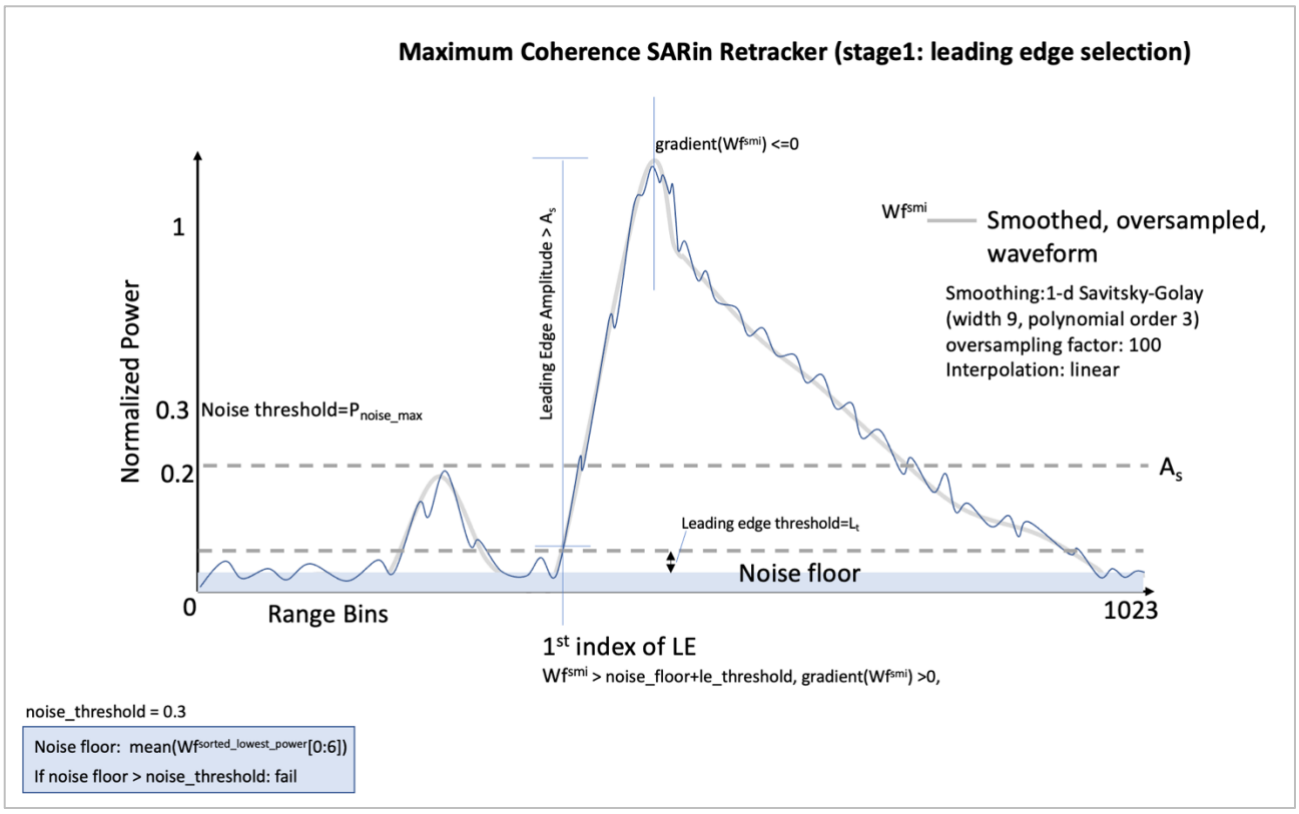

Figure 8: Schematic description of the MC Retracker's Leading Edge Selection.

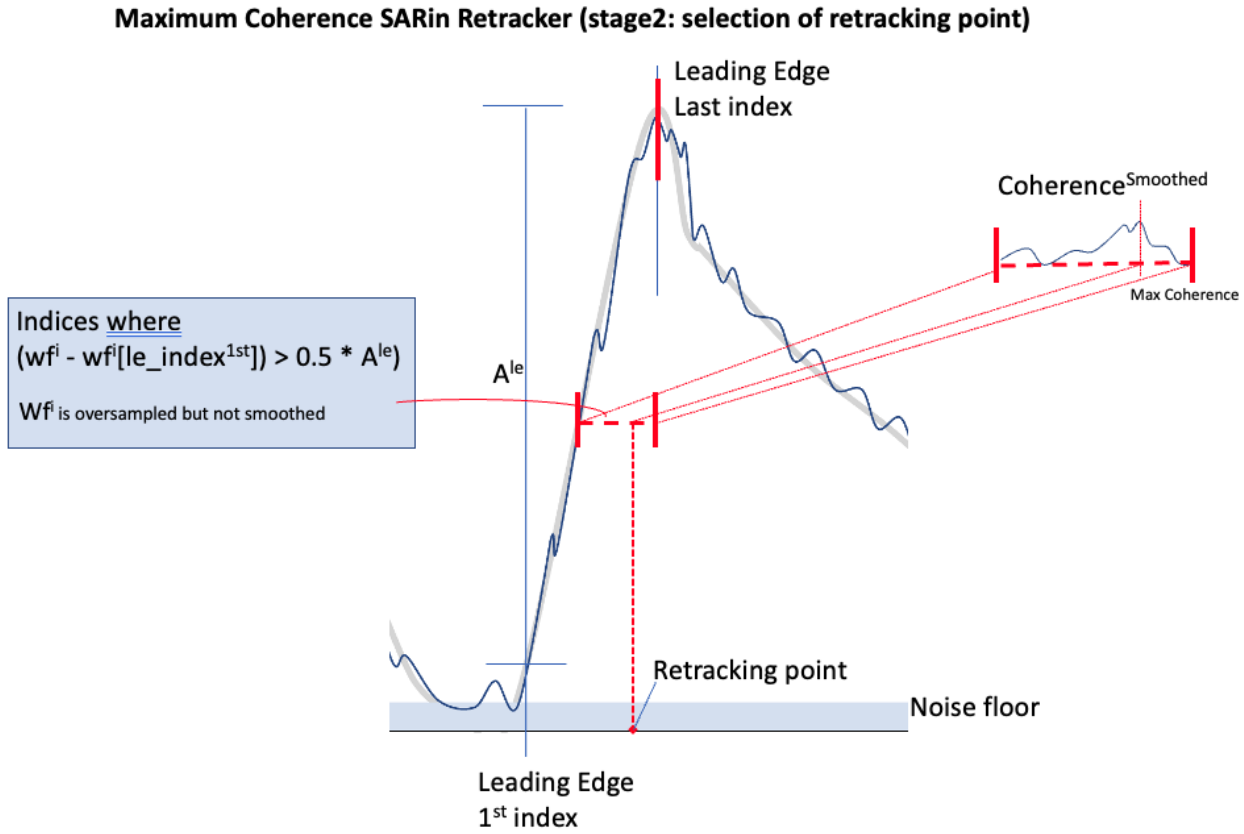

Figure 9: Schematic description of the MC Retracking Point Selection.

The specific implementation of the Maximum Coherence retracker for the Cryo-TEMPO Land Ice processor uses the following tuneable parameters and processing steps:

5.2.2.2 Tuneable Constants

Tuneable Parameter	Symbol	Value
Speed of Light	C	299792458 m/s
Chirp bandwidth	B	320000000 Hz
Waveform Oversampling Factor	W_s	100
Noise Sampling Limit	N_s	6
Noise threshold	P_{noise_max}	0.3
Leading Edge Threshold	L_t	0.05
Leading Edge Normalised Amplitude Threshold	A_s	0.2
Savitsky-Golay Smoothing width	S_w	9
Savitsky-Golay Polynomial Order	S_p	3

Coherence Smoothing Width	C_w	9
SARin Reference bin number	I_{ref}	512
Range bin size	R_b	C/(2B) for LRM C/(4B) for SIN

5.2.2.3 Retracking Method

The following retracking steps are applied to each waveform:

1. Compute maximum amplitude of waveform power, *P*.

2. Compute Normalised waveform, P_n, so that maximum amplitude is 1.

3. Apply a Savistky-Golay smoothing filter (polynomial order=S_p, width=S_w) to the waveform, forming P_{n_smooth}.

4. Compute thermal noise, P_{Noise}, from first N_s samples of normalised waveform. P_{Noise} is defined as:

$$mean(P_n[0:N_s])$$

5. Reject the waveform if the thermal noise is greater than threshold P_{noise_max}.

6. Over-sample the normalised waveform P_n and normalised smoothed waveforms P_{n_smooth} by the over-sampling factor W_s using 1-d linear interpolation, forming P_{n_i} and $P_{n\_smoothed\_i}$.

7. Compute the first derivative, *D*, of the smoothed waveform $P_{n\_smooth\_i}$ using a central difference which is calculated between *i-1:i+1*. The gradient is computed using second order accurate central differences in the interior points and first order accurate one-sides (forward or backwards) differences at the boundaries.

8. Perform an iterative search for a suitable leading edge, where the peak is greater than the amplitude threshold A_s:

   a. Find $i_{leading\_edge\_start}$, the first index of the waveform where:

$$P_{n\_smooth\_i} > (P_{noise\_max} + L_t)$$

   and

$$D_i > 0$$

b. Find i_{peak} where the gradient D_i first becomes negative after the power threshold is exceeded.

c. Calculate the amplitude of the peak:

$$A_{peak} = i_{peak} - i_{leading\_edge\_start}$$

d. If $A_{peak} > A_s$ then go to next step (leading edge is found), else continue search for leading edge.

9. The leading edge has now been identified, so find the retracking point using point of maximum coherence in the top half of the leading edge:
   a. Smooth the Coherence waveform using a running average window of width C_w
   b. Find index $i_{50\%}$ of 50% of the power up the leading edge to start search for maximum coherence.
   c. Find index of maximum coherence i_{max_coh} between $i_{50\%}$ and the first peak of the leading edge.

10. Compute range offsets from reference to retracked bins:

$$i_{offset} = i_{\max\_coh} - i_{ref}$$

11. Convert range offset to m:

$$R_{offset} = i_{offset}\, R_b$$

12. Store power in counts at retracking point (used for backscatter calculation):

$$P_{rtr} = P\left[i_{\max\_coh}\right]$$

5.3 Backscatter

The form of the backscatter (sig0_20_ku) computation is presented in [RD4] §4.5, so for the full details the reader is referred to RD4. The amplitude (determined by the TCOG retracker) is converted to a power in watts using the scaling factors (echo_scale_factor_20_ku, echo_scale_pwr_20_ku) in the L1b product.

For SARIn mode, an adjustment is made to the geometry as given in §4 of [RD5].

(rx_power, transmit_pwr_20_ku, range) ---> (sig0_20_ku)

It should be noted that SARin mode backscatter values calculated for CryoTEMPO Baseline-B will be on average 2dB higher than those calculated in Baseline-A. This is not a fixed bias but the result of the change in SARin retracker in Baseline-B, which selects a retracking point on average higher up the leading edge.

5.4 Slope Correction (LRM)

The LRM slope correction algorithm uses pre-computed grids of range slope to compute the attitude (angle from nadir) and azimuth (angle from x-axis of grid) of a vector from the satellite to the slope corrected location in the slope model frame of reference. The full details of the algorithm are presented in [RD4] §4.6, and so for the full details the reader is referred to RD4.

(lon_20_ku, lat_20_ku) ---> (attitude, azimuth)

5.5 Elevation and POCA Computation (LRM)

The elevation and POCA computation algorithms compute the geodetic height (z_e in Figure 10) and location of the endpoint of a vector projected from the satellite in the attitude (η) and azimuth direction (ϕ), for the measured range (l). As a difference in range means a difference in location, only one of the range estimates must be chosen to provide the location. The details of the algorithm are presented in [RD4] §4.7, and so for the full details the reader is referred to RD4.

(attitude, azimuth, alt_20_ku, range_cor_tcog_20_ku) ---> (lat_poca_20_ku, lon_poca_20_ku, height_tcog_20_ku)

(attitude, azimuth, alt_20_ku, range_cor_tfmra_20_ku) ---> (height_tfmra_20_ku)

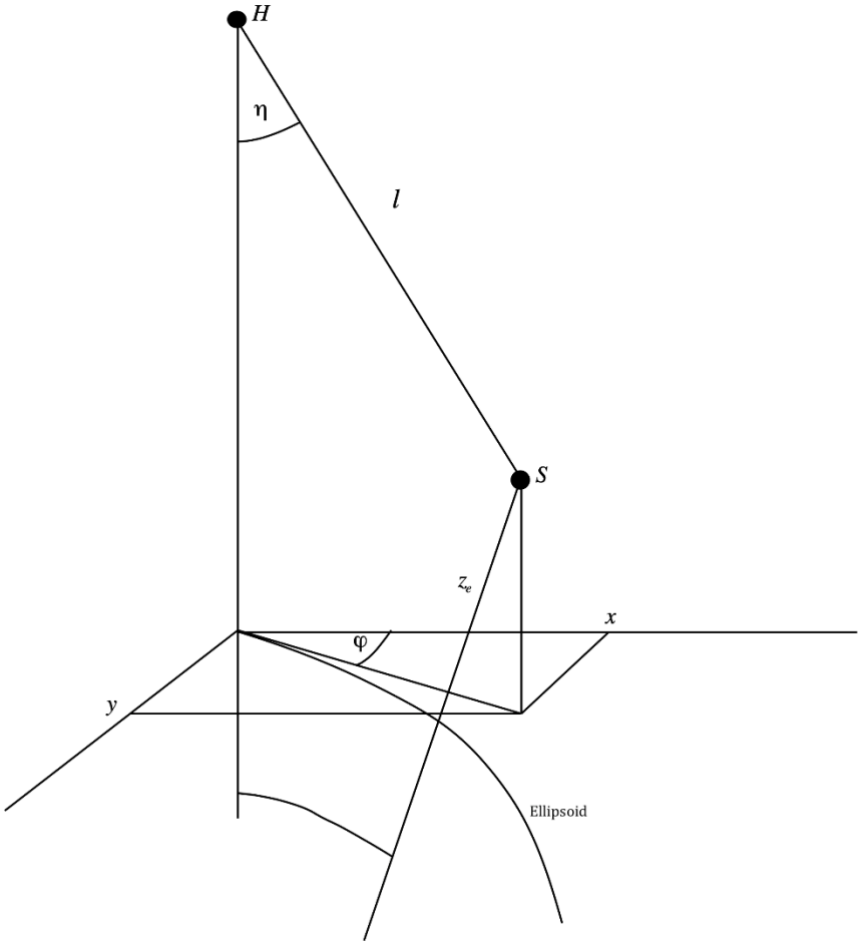

Figure 10: Geometry of LRM elevation computation.

5.6 Slope Doppler Correction (LRM)

If the POCA location is not purely across-track, there is a component of the satellite velocity in the direction of the vector from the satellite to the POCA location. This necessitates a delta-doppler correction to the range (and therefore to the height). Details of the algorithm are presented in [RD4] §4.8, and so for the full details the reader is referred to RD4.

(lat_20_ku, lon_20_ku, alt_20_ku, sat_vel_vec_20_ku, lat_poca_20_ku, lon_poca_20_ku, height_tcog_20_ku) ---> (height_tcog_20_ku')

(lat_20_ku, lon_20_ku, alt_20_ku, sat_vel_vec_20_ku, lat_poca_20_ku, lon_poca_20_ku, height_tfmra_20_ku) ---> (height_tfmra_20_ku')

5.7 Across-track Angle Computation (SARIn)

A window is extracted from the phase difference waveform, symmetrically about the retracking location.

N is the number of bins in the phase window and N is an even number.

$$phase\_window = ph\_diff\_waveform[floor(ind\_wfm\_retrack\_20\_ku) - {}^{N}/_{2} : floor(ind\_wfm\_retrack\_20\_ku) + {}^{N}/_{2}]$$

The SARin phase difference waveform is now sampled **at the location of maximum coherence** chosen by the retracker (instead of using a model fit in Baseline-A). No smoothing or interpolation is performed. The phase difference value is then converted into an angle from the boresight vector (given in the L1 data), using the method described in [RD4] §6.5.

5.8 Elevation and POCA Computation (SARIn)

The elevation and POCA algorithm computes the geodetic height and location of the endpoint of a vector projected from the satellite in the across-track direction, for the measured range at the across track angle. As a difference in range means a difference in location, only one of the range estimates must be chosen to provide the location. The details of the algorithm are presented in [RD4] §6.5, and so for the full details the reader is referred to RD4.

(sat_vel_vec_20_ku, inter_base_vec_20_ku, alt_20_ku, across_track_angle, range_cor_tcog_20_ku) ---> (lat_poca_20_ku, lon_poca_20_ku, height_tcog_20_ku)

(sat_vel_vec_20_ku, inter_base_vec_20_ku, alt_20_ku, across_track_angle, range_cor_tfmra_20_ku) ---> (height_tfmra_20_ku)

In Baseline-A an ambiguity check was performed to detect potential phase wrapping by comparing the measured SARin height with an external DEM. Differences greater than 100m were flagged as ambiguous but no attempt was made to correct the measurements location and elevation.

In Baseline-B to determine if the original phase measurement was wrapped, the phase difference is then unwrapped and a second elevation and location is calculated. The location with the smallest difference from the DEM is taken as the POCA and the height measurement is given at that location. This results in the retrieval of a higher number of SARin measurements over the ice sheet margins in Baseline-B.

5.9 Basin ID

For each 20 Hz measurement over land ice surfaces, a glaciological catchment basin identifier is assigned, the purpose of which is to allow the user to easily filter by – and extract data from – a specific basin or catchment of interest.

In Baseline-B, two different glaciological basin identifiers are provided for each measurement as defined by Zwally (2012) and Rignot (2016). These represent the two most common current methods of defining ice sheet basins, and are both used in the Ice Sheet Mass Balance Intercomparison Exercise (IMBIE; http://imbie.org/), thereby allowing the user to easily extract data over a consistent region to the IMBIE datasets.

For Antarctica, the ice sheet is split into 27 distinct basins, using the Zwally Antarctica basin definition (Zwally *et al.*, 2012) and in to 18 basins for the Rignot definition. For Greenland, the ice sheet is split into 19 distinct basins, using the Zwally Greenland basin definition (Zwally *et al.*, 2012) and 6 basins using Rignot. These basins can be downloaded directly from http://imbie.org/imbie-2016/drainage-basins/.

Zwally (2012) Basins

Rignot (2016) Basins

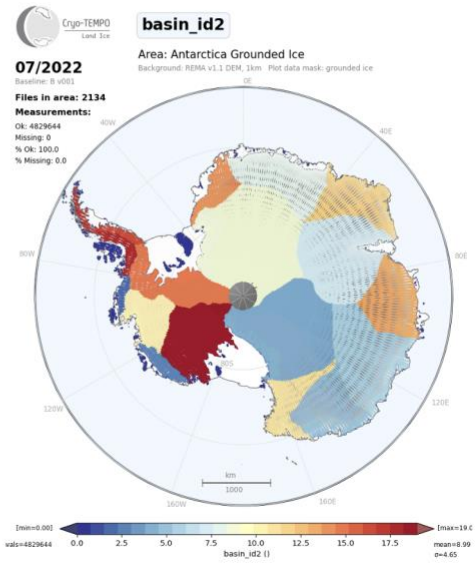

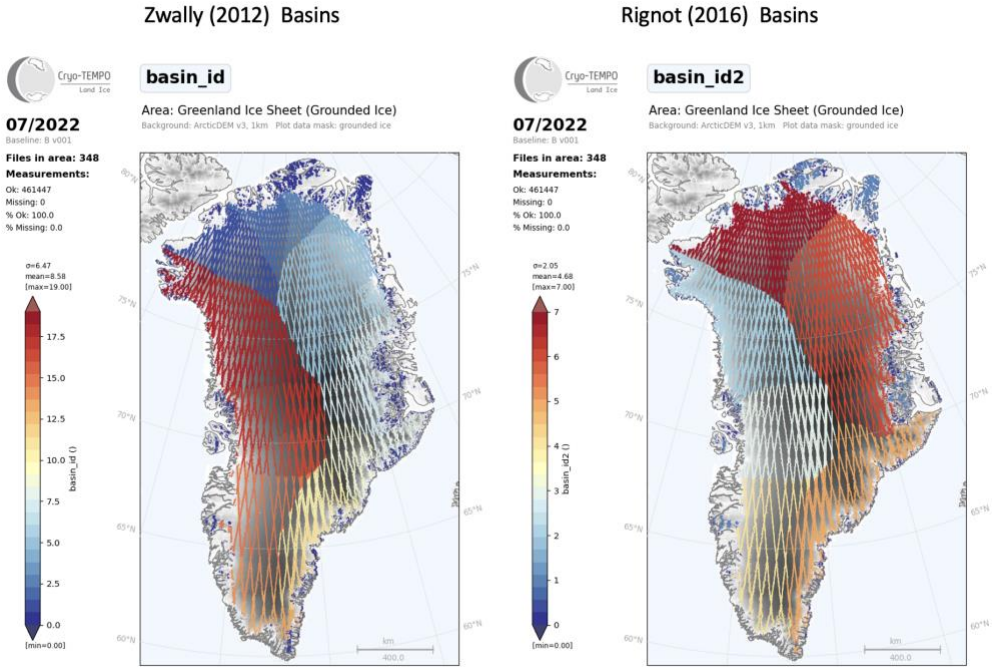

The basin ID masks are netCDF format grids of basin ID in stereographic projection. They are indexed by nearest neighbour to retrieve the basin ID at the POCA location.

(X_0, Y_0) = grid corner from netCDF file
Step = grid spacing from netCDF file
(lon_20_ku, lat_20_ku) ---> (X,Y)

$$basin\_id\_20\_ku = grid\left[round\left(\frac{X - X_0}{step}\right), round\left(\frac{Y - Y_0}{step}\right)\right]$$

5.10 Uncertainty estimation

The uncertainty estimate comes from an empirical parameterisation based on the ice sheet surface slope. The magnitude of the surface slope at the POCA lat/lon is computed by reference to a slope map. The uncertainty estimation table is indexed by the retrieved slope magnitude and the retrieved estimate of uncertainty is placed into the output product. The method of uncertainty calculation within each band of surface slope is described in section 6.

5.11 DEM height

The reference DEMs are netCDF format grids of elevation in polar stereographic projection. Elevation units are meters and are referenced to the WGS84 ellipsoid.

5.11.1 Input Antarctic DEM data

For Antarctica, the REMA 1km Mosaic DEM v1.1 is used.

The source link to the data is:
http://data.pgc.umn.edu/elev/dem/setsm/REMA/mosaic/v1.1/1km/REMA_1km_dem_filled.tif.

REMA mosaics are provided in the EPSG:3031 projection.

5.11.2 Input Greenland DEM data

For Greenland, the ArcticDEM (v3.0) 1km Mosaic is used.

The source link to the data is:
http://data.pgc.umn.edu/elev/dem/setsm/ArcticDEM/mosaic/v3.0/1km/arcticdem_mosaic_1km_v3.0.tif.

It is provided in the EPSG:3413, Polar Stereographic North projection.

5.11.3 Null Values

The DEM data may contain void pixels where no elevation measurement exists. Data voids may be present where the source imagery contains cloud cover or shadowed areas. The void areas contain null values (-9999) in lieu of the terrain elevations. In these cases, for each Cryo-TEMPO measurement, a linear interpolation of the surrounding data is performed to calculate the DEM height.

6 UNCERTAINTY ESTIMATE TABLE CREATION

As described in Section 5.10, the uncertainty associated with each measurement is extracted from an uncertainty table. This table is indexed by the slope magnitude and gives the associated uncertainty in the height estimate expected for a slope of that magnitude. The uncertainty estimate is then placed into the output product.

In this section, the method for creating the uncertainty table is described further. The basic assumption made in this version of the data product is that the uncertainty is only dependent on surface slope. For future versions, this will be expanded to include other relevant parameters such as e.g. complex multi-peaked waveforms, anisotropic backscattering and variations in the depth distribution of scattering elements; i.e. radar penetration, if they are found relevant in our further analysis.

The slope correction applied to the radar altimeter (RA) measurement introduces an error that is found to dominate over the pure measurement error over topographically inclined surfaces (Bamber et al., 1994), and the assumption of a slope-dependent uncertainty is well-described and documented in the literature already, e.g. Schröder et al., 2019 and McMillan et al., 2019.

Our approach is an empirical one, that is designed to adequately characterise the uncertainty given the unique complexity that affects elevation retrievals over land ice.

6.1 Data used for Uncertainty Calculation

In order to estimate the uncertainty of Cryo-TEMPO elevation measurements in different bands of surface slope, we find the median absolute differences of Cryo-TEMPO elevation to a known external source of surface elevation validation data which is known to have a high accuracy (< 3.3cm) and precision (< 7cm) over the ice sheets.

The primary source of data for evaluating radar altimetry missions was previously height data derived from Operation IceBridge airborne campaigns (2009-2019). This airborne mission was followed by ICESat-2, which launched in September 2018 and provides a similar quality of validation data from its ATLAS lidar instrument, albeit with greatly improved spatial and temporal coverage. ICESat-2 measurements are now available over the whole Antarctic and Greenland ice sheet below 88° north and south with a 90 day repeat.

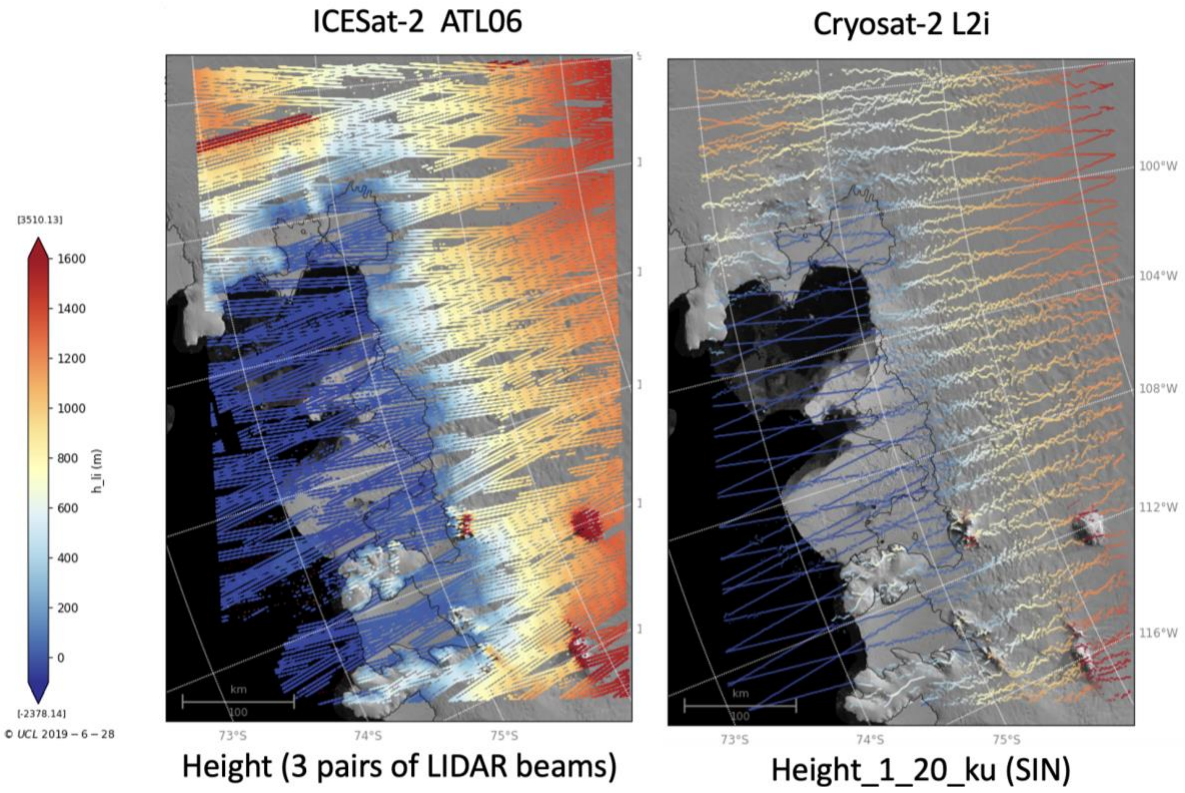

Figure 11: Comparative measurement coverage of ICESat-2 (2018-, 90-day repeat) and CryoSat-2 (2010-, 30-day sub-cycle)

ICESat-2's Advanced Topographic Laser Altimeter System (ATLAS) measures the ice surface with high accuracy and precision using 6 lidar beams arranged as 3 pairs.

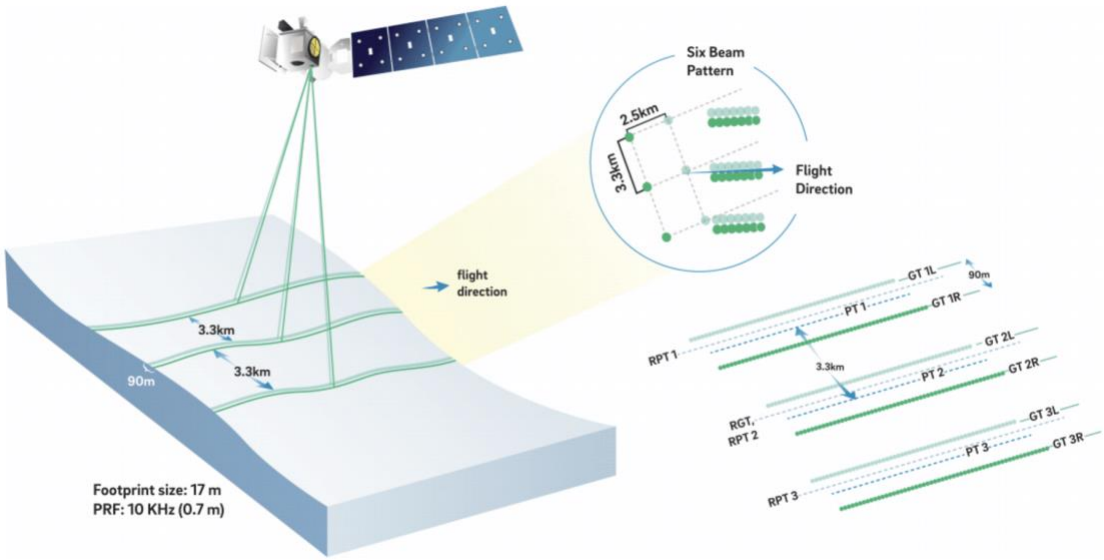

Figure 12: ICESat-2 beam arrangement (B. Smith, 2019)

Validation studies using comparison with GNSS such as Brunt et al, 2019; 2021, have shown that ATL06 is currently accurate over the ice sheet interior to better than 3.3 cm, with better than 7.2 cm surface measurement precision. Li et al, 2021 also demonstrated an accuracy of 1.5cm with a precision of 9.1cm over a test zone covering a variety of Antarctic ice surface conditions along the 520 km traverse.

6.2 Method of Cryo-TEMPO Uncertainty Calculation

We estimate the accuracy of the Cryo-TEMPO elevation measurements by calculating the point to point differences between Cryo-TEMPO elevations and those from all 6 beams of ICESat-2 ATL-06 v005, which are co-located within a 20m search radius.

In order to minimize the effects of actual (temporal, dz/dt) surface elevation changes between the two profiles, we restrict the time differences between Cryo-TEMPO CS2 and IS2 ATL06 measurements to less than 1 month.

For each point to point location found, we extract the magnitude of the surface slope from an external file (ArcticDEM or REMA), and use one full year of monthly (CryoTEMPO-ICESat-2) height differences to build the look-up table containing binned estimates of corresponding slope and uncertainty (sigma). Hence, we assume that the uncertainty (slope) is stationary in time, which is a reasonable assumption from a geophysical perspective. The median absolute difference is derived from all the differences obtained within each slope bin. If no value is available within a given bin (e.g. due to low data volumes at a given slope), the bin value is estimated from linear interpolation of the surrounding bins.

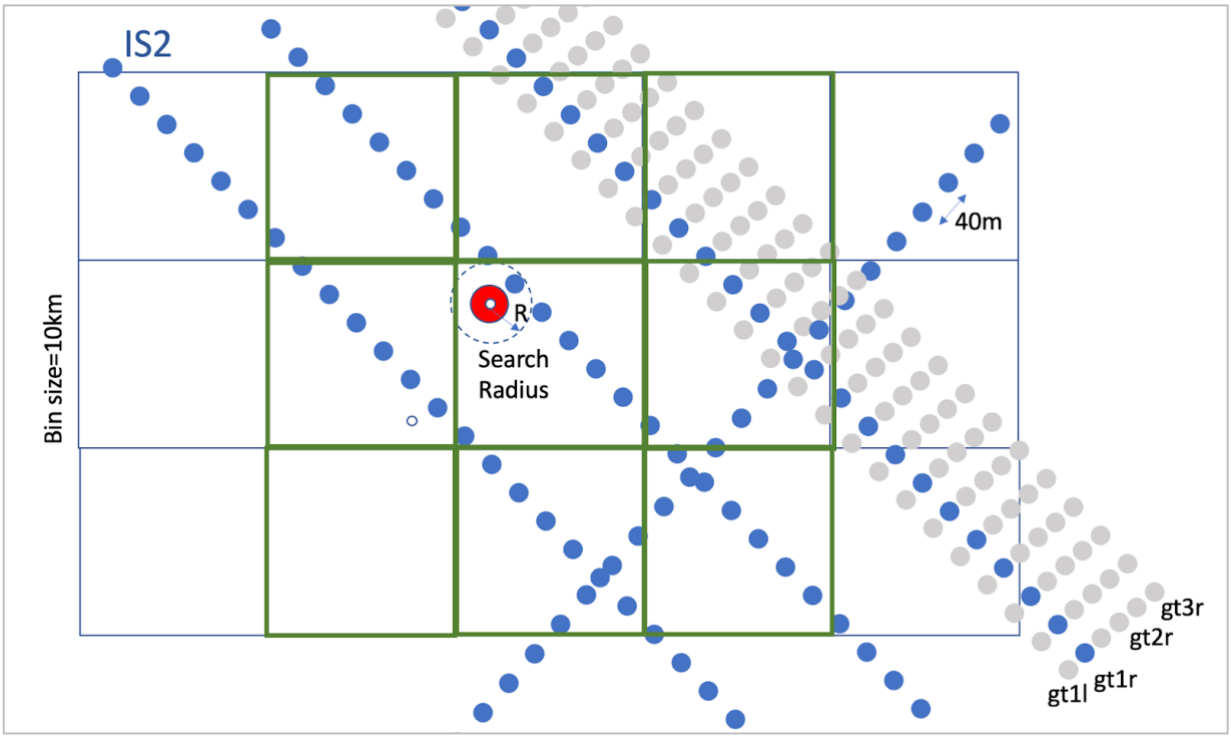

Figure 13: Point to Point Differences found between CS2 (red dot) and ICESat-2 ATL-06 elevation measurements (blue and grey dots) located within a 20m radius and with a time difference of less than 1 month. The differencing method used first grids both data sets in to a 10km grid and only searches for collocated measurements within each grid cell and immediate neighbours.

The workflow of the method is as follows.

A representative year is selected which contains full coverage from both CryoSat-2 and ICESat-2. In this case we choose 2020 (a year in which we have full coverage from CryoSat and ICESat-2).

For each month of selected year:

For each ICESat-2 beam (Gt3l,Gt3r,Gt2l,Gt2r,Gt1l,Gt1r):

1. Select all ICESat-2 elevation measurements from selected beam that are located within the Cryo-TEMPO land ice area of interest (Greenland or Antarctica mask).
2. Grid selected IS2 ATL-06 elevation measurements in to a 10kmx10km polar stereo grid.
3. For each Cryo-TEMPO elevation measurement in this month, search the grid cell and surrounding grid cells for ICESat-2 measurements within a 20m radius. If found store the CS2-IS2 elevation difference and location of the CS2 measurement, and the local surface slope interpolated from a slope map (derived from an external REMA or ArcticDEM DEM).

From all the (*dH, slope*) pairs found within the full year of data:

1. The median absolute difference, *m*, of the *dH* values within each slope bin (0.1° steps, between 0 and 2°) are derived.
2. A table of binned (*m, slope*) values is created. If bin values are missing then these are linearly interpolated from surrounding bins.

For all Cryo-TEMPO measurements, the associated surface slope at that measurement location is extracted, and the look-up table is used to derive the associated uncertainty.

7 KNOWN ISSUES

There are several known assumptions, limitations and anomalies in the ice sheet elevation retrieval process that affect the fidelity and certainty of the variables in the Cryo-TEMPO Land Ice product. The primary limiting assumptions are summarised as follows:

- Identification of the true echoing point in Low Resolution Mode (LRM). In LRM, the 'angle of arrival' between the satellite boresight and the surface reflection point (usually assumed to be the Point of Closest Approach) is not measured directly and is instead approximated based upon an auxiliary slope model, derived from a Digital Elevation Model. Inaccuracies in the DEM, or in the assumption that the retracking point identifies the Point of Closest Approach, can therefore lead to errors in the derived elevation.

- Penetration of the radar wave into the near surface snowpack. The degree of penetration of the radar wave into the snowpack is spatially and temporally variable, meaning that derived elevations do not always correspond to the true air-snow interface. This can complicate the interpretation of Ku-band altimeter elevation measurements, for example when they are compared to laser altimeter observations.

- Onboard tracking. Over very complex terrain, such as narrow outlet glaciers surrounded by high mountain peaks, the altimeter's onboard tracker can fail to keep track of the ice surface (so called 'loss of lock'). This can occasionally lead to irretrievable loss of data over regions such as the Antarctica Peninsula.

- LRM Backscatter (sigma0). There is a known drift and step in the CryoSat ESA Baseline-D/E L1b parameters used to calculate sigma0 for LRM measurements. Correction of this drift is a L1b process and is beyond the scope of the Cryo-TEMPO project, and cannot be corrected until CryoSat ESA Baseline-E is fully processed for the full mission (scheduled for 2023).

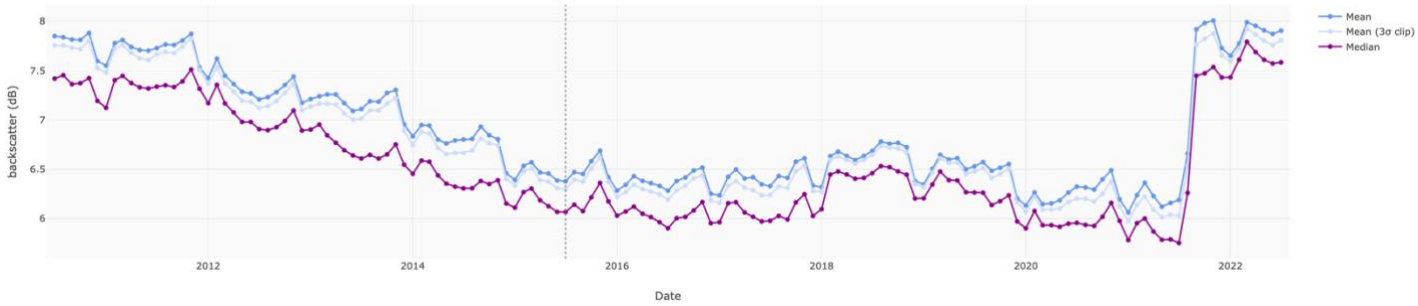

Figure 14: Drift in Backscatter for LRM mode

For a full summary of all known anomalies in the ESA L1b ice chain, the reader is referred to the CryoSat Ice Data Quality Status Summary (https://earth.esa.int/documents/10174/129120/CryoSat-Ice-Product-Status.pdf).

8 REFERENCES

Aublanc,J.;Thibaut,P.; Guillot, A.; Boy, F.; Picot, N. Ice Sheet Topography from a New CryoSat-2 SARIn Processing Chain, and Assessment by Comparison to ICESat-2 over Antarctica. Remote Sens. 2021,13,4508. https://doi.org/ 10.3390/rs13224508

Bamber, J. L. (1994). Ice sheet altimeter processing scheme. *International Journal of Remote Sensing*, *15*(4), 925-938.

Brunt, K. M., Neumann, T. A., and Smith, B. E.: Assessment of ICESat-2 ice sheet surface heights, based on comparisons over the interior of the Antarctic ice sheet, Geophys. Res. Lett., 46, 13072–13078, https://https://doi.org/10.1029/2019GL084886, 2019b.

Brunt, K. M., Smith, B. E., Sutterley, T. C., Kurtz, N. T., and Neumann, T. A.: Comparisons of Satellite and Airborne Altimetry With Ground-Based Data From the Interior of the Antarctic Ice Sheet, Geophys. Res. Lett., 48, e2020GL090572, https://doi.org/10.1029/2020GL090572, 2021.

Helm, V., a. Humbert, and H. Miller (2014), Elevation and elevation change of Greenland and Antarctica derived from CryoSat-2, Cryosph., 8(4), 1539–1559, doi:10.5194/tc-8-1539-2014.

Li, R., Li, H., Hao, T., Qiao, G., Cui, H., He, Y., Hai, G., Xie, H., Cheng, Y., and Li, B.: Assessment of ICESat-2 ice surface elevations over the Chinese Antarctic Research Expedition (CHINARE) route, East Antarctica, based on coordinated multi-sensor observations, The Cryosphere, 15, 3083–3099, https://doi.org/10.5194/tc-15-3083-2021, 2021.

McMillan, M., Muir, A., Shepherd, A., Escolà, R., Roca, M., Aublanc, J., Thibaut, P., Restano, M., Ambrozio, A. and Benveniste, J.: Sentinel-3 Delay-Doppler altimetry over Antarctica, Cryosphere, 13(2), 709–722, doi:10.5194/tc-13-709-2019, 2019.

Schröder, L., Horwath, M., Dietrich, R., Helm, V., Broeke, M. R., & Ligtenberg, S. R. (2019). Four decades of Antarctic surface elevation changes from multi-mission satellite altimetry. *The Cryosphere*, *13*(2), 427-449.

Wingham, D., A. Ridout, R. Scharroo, R. Arthern, and C. Shum (1998), Antarctic elevation change from 1992 to 1996, Science (80-.)., 282(5388), 456–458.

Zwally, H. Jay, Mario B. Giovinetto, Matthew A. Beckley, and Jack L. Saba, 2012, Antarctic and Greenland Drainage Systems, GSFC Cryospheric Sciences Laboratory, at http://icesat4.gsfc.nasa.gov/cryo_data/ant_grn_drainage_systems.php.